Int j simul model 23 (2024) 2, 275-286
Original scientific paper

MODELLING AND INVESTIGATION OF A DRIVER SEAT SUSPENSION WITH NEGATIVE STIFFNESS STRUCTURE

Turan, M. K.[*,**]; Erzan Topcu, E.[*] & Karpat, F.[*]
[*] Bursa Uludağ University, Faculty of Engineering, Department of Mechanical Engineering, Bursa, Turkey
[**] Grammer Koltuk Sistemleri San. ve Tic. A.Ş. Bursa, Turkey
E-Mail: mkivancturan@uludag.edu.tr, erzan@uludag.edu.tr, karpat@uludag.edu.tr

Abstract
In this study a narrow suspension seat with negative stiffness structure (NSS) was investigated. First, this suspension seat's fundamental equations were detected, and then a simulation model was created using Altair Inspire software and validated by a literature study. Inspire software was used for the first time for suspension seat with NSS in the literature vis-a-vis the authors' literature search. Afterward, the case design was created via the Taguchi method to determine parameter effects of NSS of suspension seat. Signal-to-noise ratio (S/N) and ANOVA were used to examine simulation results, thus, parameter effects of NSS of suspension seat were examined comprehensive statistically for the first time in the literature vis-a-vis the authors' literature search. Therefore, it was seen that the spring ratio is a much more effective parameter than the spring preload value for vibration isolation. In addition, optimal parameters of NSS were detected. Finally, with frequency response and road input results, it was observed that the suspension seat with NSS, which crated via optimal values, showed much better isolation performance than the other passive suspension seat.
(Received in February 2024, accepted in April 2024. This paper was with the authors 2 weeks for 1 revision.)

Key Words: Vibration, Suspension Seat, Negative Stiffness Structure, ANOVA, Taguchi

1. INTRODUCTION

Vibration in vehicles is an undesirable phenomenon in terms of driving comfort and driving safety. For this reason, it is seen that the studies on the development of vibration isolation and control systems continue today [1-3]. Some of these vibrations are undesirable and need to be isolated [4]. One of the most important reasons for this is that vibration has high probability of causing damage to structures, driver, and passengers. Also, exposure to whole-body vibration for human beings is a very hazardous situation [5-10]. Vibration isolation for the drivers is critical in large vehicles such as buses and trucks. Since they drive for long periods, they are exposed long-term vibration. In addition, some vehicles are exposed to high vibration because of working conditions for instance construction equipment. Long-term exposure to whole-body vibration may cause various physical disorders for these vehicle drivers [5-10]. Because of this situation, additional isolation equipment's are needed. Therefore suspension seats are used for driver seats in such vehicles. Suspension seats can be classified as passive, semi-active and active, similar to vehicle suspensions, according to their suspension. Although semi-active and active suspension seats have high isolation performances, passive suspension seats are still more widely used due to the cost advantage. The most significant disadvantage of passive suspension seats is their limited isolation performance. The primary performance constraint of passive suspension seats is that specifications of elements are constrained, and they cannot react according to the excitation vibration. Although optimization solutions have been used [11], more effective solutions have been sought for the passive suspension seats.

Basically, if a seat suspension is considered as single degree of freedom system containing a mass, spring and damper elements, and the damping coefficient (c) is low, the stiffness of the spring (k) and the mass of the seat element (m) are the most influential parameters of the isolation performance. Because there is a relationship between the natural frequency and the

isolation starting point. In a single degree of freedom structure, the natural frequency is a function of stiffness of the spring and mass ($\omega_n = \sqrt{k/m}$). The isolation starting point is √2 times the natural frequency. To move the isolation starting point back, it is necessary to decrease the natural frequency. The ideal solution for reducing the natural frequency is to reduce the stiffness of the spring element. Nowadays, NSS are the most critical solution for this purpose. NSS are usually developed with springs or pre-buckled beams [12], some metamaterials have negative stiffness [13] also. NSS to the suspension system reduces the dynamic stiffness of the suspension. Thus, the natural frequency value decreases, and the isolation starting point is moved back. There are many interesting studies about developing NSS and adding to seat suspension. Li et al. [12] conducted a comprehensive review of NSS. Liao et al. [14] theoretically discussed the suspension seat with an NSS. Papaioannou et al. [15] investigated the performance of one passive isolator and four different negative stiffness isolators in their study. Lee et al. [16] developed a seat vibration isolator by producing negative stiffness springs from thin sheets and successfully tested it in many different vehicles. Oyelade [17] used Euler Beams for the NSS. Le and Ahn [18] discussed the NSS in the vehicle seat. Firstly, the NSS was discussed theoretically, and then numerical and experimental work was carried out. As a result of the study, it was seen that the NSS has a positive effect on the isolation performance. Le and Ahn in their study [19], which is a continuation of their work in 2011, also included the size of the horizontal spring compression element in their calculations. In another study, Le and Ahn [20] focused on an active isolator. Similar to the passive vibration isolator, it has been observed that the NSS increases performance in the active vibration isolator. Rahman and Rahman [21] discussed the single or dual use of NSS. As a result of study, it was observed that dual using of NSS provided better isolation performance. Ma et al. [22] conducted a comprehensive review study on the quasi-zero stiffness mechanism. Some studies were focused on the parameter's optimization of the NSS [23, 24].

In this study, a new NSS was developed for the existing suspension driver seat system and adapted to this suspension seat. Thus, an original and low-cost suspension seat with NSS was created. Firstly, the basic static and dynamic motion equations of the NSS was investigated and validated with a literature study. Based on the validated numerical model, the isolation performance of the new suspension seat with NSS was investigated numerically. First of all, a simulation model of this driver seat suspension system with NSS was established using Altair® Inspire software. With this program, the compatibility of the negative stiffness system using with the seat suspension system and dynamic behaviour of this system was evaluated. The study is precious in showing the availability of Inspire software for vibration simulation. Afterwards, a case set was created with the help of Taguchi method to determine the effects of the parameters selected for this study. The obtained results were also analysed by signal-to-noise ratio and ANOVA. Thus, the isolation results of the suspension seat with NSS were investigated comprehensively statistically for the first time in the literature vis-a-vis the authors' literature search.

2. MATERIAL AND METHOD

As you can see in Fig. 1, the suspension seat with NSS system contains nine essential parts. These are two horizontal springs, two bars, two compression parts, a vertical spring, a mass, and scissors. These elements are standard machine elements or simple structured parts; thus, production costs are low.

The task of the scissors is to ensure that the mass moves only in the vertical direction and to restrict its freedom in other directions. Bars and horizontal springs create the NSS, while compression parts compress the horizontal springs and act as joints for the bars.

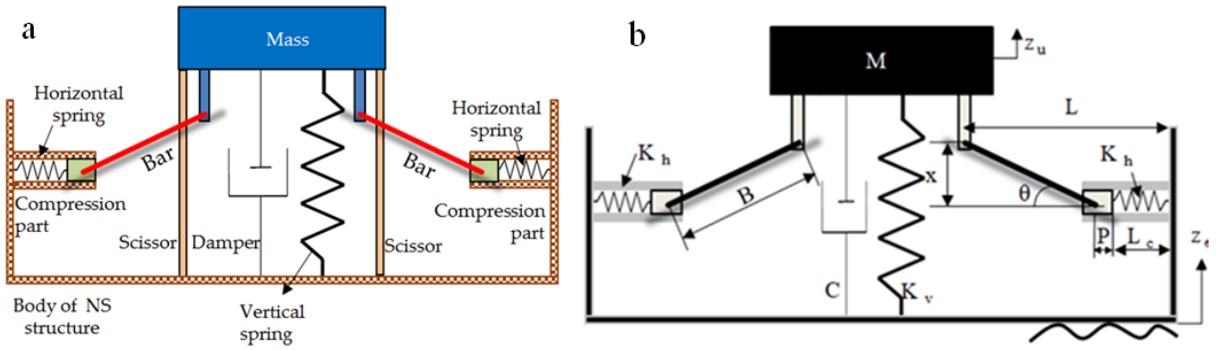

Figure 1: Seat suspension with NSS, a) elements of suspension, b) parameters of suspension.

The design developed in the study (Fig. 1) is narrower than the designs of many studies in the literature. Since corner zones are preferred for mass joint connection points in literature designs generally, thus the width of the suspension seat is increased by the total size of the bar, compression part, and compressed length of the horizontal spring. The critical point in the design of NSS is to move the joint connection points. Thus, the structure was narrowed without any deviation from the values targeted by the calculations. However, there are two limitations: Firstly, joint connection points could not contact with damper or vertical spring. Secondly, the mass could not contact with the other parts such as bar, compression part, raceway of compression part. In the design carried out for the study, a width reduction of 110 mm was achieved with this design method and limitations. Fig. 1 b shows Seat suspension parameters.

In Fig. 1 b, when the mass moves vertically, the total force occurring in the springs is expressed as in Eq. (1) [19].

$$F = F_v + 2F_h \tan\theta \tag{1}$$

Here, F_v denotes the force in the vertical spring, while F_h denotes the force in the horizontal springs. *tan* θ means the slope of the bar [19].

$$tan\,\theta = \frac{x}{\sqrt{(B^2 - x^2)}} \tag{2}$$

Here, B is bar length and x is the displacement of the mass relative to the suspension body. If the forces in Eq. (1) are written in terms of spring stiffness and compression length [19];

$$F = K_v x + 2K_h \left(L - P - \sqrt{B^2 - x^2} - L_f\right) \frac{x}{\sqrt{(B^2 - x^2)}}$$

$$F = K_v x + 2K_h \left(\frac{L - P}{\sqrt{B^2 - x^2}} - \frac{L_f}{\sqrt{B^2 - x^2}} - 1\right) x \tag{3}$$

Here, L is the horizontal distance of mass connection point, L_f is the length of the spring in the free-state, P length of compression part, K_v stiffness of vertical spring, and K_h stiffness of horizontal spring. The non-dimensionalization of the force equation provides a better understanding of the parameter effects. Various parameters were created to obtain the dimensionless force [19].

$$\bar{F} = \frac{F}{K_v L_f}, \bar{x} = \frac{x}{L_f}, \gamma_1 = \frac{B}{L_f}, \gamma_2 = \frac{L - P}{L_f}, \alpha = \frac{K_h}{K_v} \tag{4}$$

Here, $\bar{F}$ is the dimensionless force, $\bar{x}$ the dimensionless displacement, α the stiffness ratio. γ_1 and γ_2 are the necessary regulation parameters for the equations [19]. α must be carefully chosen so that the horizontal spring can exert the necessary negative stiffness effect. If this ratio is lower or higher than necessary, it will cause the system to work inefficiently. γ_1 and γ_2 are related to preload of the horizontal springs. In the dynamic state, the suspension system will work inefficiently if the horizontal springs do not have the necessary preload.

$$\bar{F} = \bar{x} + 2\alpha\left(\frac{\gamma_2 - 1}{\sqrt{{\gamma_1}^2 - \bar{x}^2}} - 1\right)\bar{x} \tag{5}$$

The dimensionless stiffness $\bar{K}$ was obtained by taking the derivative of the dimensionless force with respect to the dimensionless displacement [19].

$$\bar{K} = 1 + 2\alpha\left(\frac{\bar{x}^2(\gamma_2 - 1)}{({\gamma_1}^2 - \bar{x}^2)^{\frac{3}{2}}} - \frac{(1 - \gamma_2) + \sqrt{{\gamma_1}^2 - \bar{x}^2}}{\sqrt{{\gamma_1}^2 - \bar{x}^2}}\right) \tag{6}$$

In the static state, the displacement value is $x = 0$, so the dimensionless stiffness equation can be expressed as in Eq. (7).

$$\bar{K} = 1 + 2\alpha\left(\frac{(\gamma_2 - \gamma_1 - 1)}{(\gamma_1)}\right) \tag{7}$$

As can be seen in Eq. (7), three basic parameters γ_1, γ_2, and α influence the dimensionless stiffness. The arrangement between these parameters will give the ideal dimensionless stiffness value. Applying a vertical excitation from the body of NSS, $z_e(t)$ is transmitted to the mass, M via the isolation system as shown in Fig. 1 b. The motion equation of this system can be obtained using Newton' s Second Law of motion as below.

$$\ddot{x} + \frac{C}{M}\dot{x} + \frac{K_v}{M}x - 2\frac{K_h}{M}\left(1 + \frac{1 - \gamma_2}{\sqrt{\gamma_1^2 - \frac{x^2}{L_f^2}}}\right)x = -\ddot{z}_e \tag{8}$$

Here z_u is the absolute displacement of the mass, x is the displacement of the mass relative to the to the body and can be explained $x = z_u - z_e$ as. C is the viscous damping coefficient. The absolute vibration transmissibility (T_a) can be defined as the ration of the magnitude of the absolute displacement of the mass to the body of NS system as:

$$T_a = \frac{|z_u|}{|z_e|} \tag{9}$$

This ratio is calculated using the Altair® Inspire analysis results, measuring the amplitude of the mass according to the sinusoidal input: $z_e(t) = |z_e|\sin(\omega t)$.

2.1 Validation study

As stated above, the effects of γ_1, γ_2, and α on stiffness need to be determined. At this point, a static state validation was carried out through the study of Le and Ahn [19]. Five γ_2 and four α values were selected for validation processes. The values of Le and Ahn's study were given in Fig. 2 a and Fig. 3 a and validation results of this study were given in Fig. 2 b and Fig. 3 b.

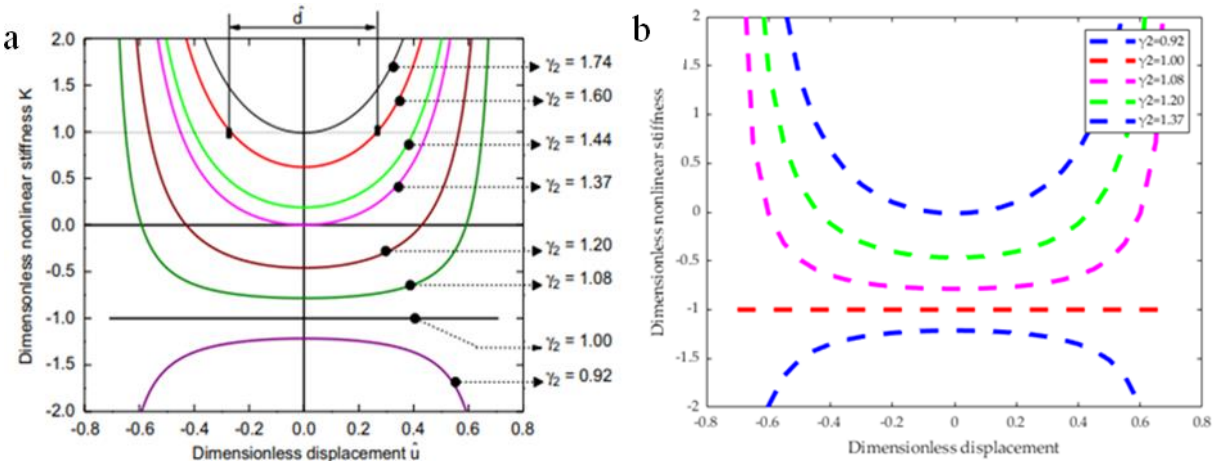

Figure 2: Validation of static characteristics for variation of γ_2 parameter ($\gamma_1 = 0.75$, $\alpha = 1$); a) Le and Ahn 2013 [19], b) validation results.

As can be seen in Fig. 2, when $\gamma_1 = 0.75$ and $\alpha = 1$, if γ_2 increases, the dimensionless nonlinear stiffness increases and moves away from zero. When this value decreases, it is seen that the dimensionless nonlinear stiffness approaches zero or even falls below zero. Another remarkable point in Fig. 2 is that the direction of the curve turns 180 degrees when the γ_2 value is lower than one. In other words, the curve peaks when the dimensionless displacement value is 0. One of the critical points in these curves is the effective dimensionless displacement value, that is, the range where the dimensionless stiffness is less than one. The larger this value, indicated by $\hat{d}$ in Fig. 2 a, the wider the operating range of the negative stiffness system.

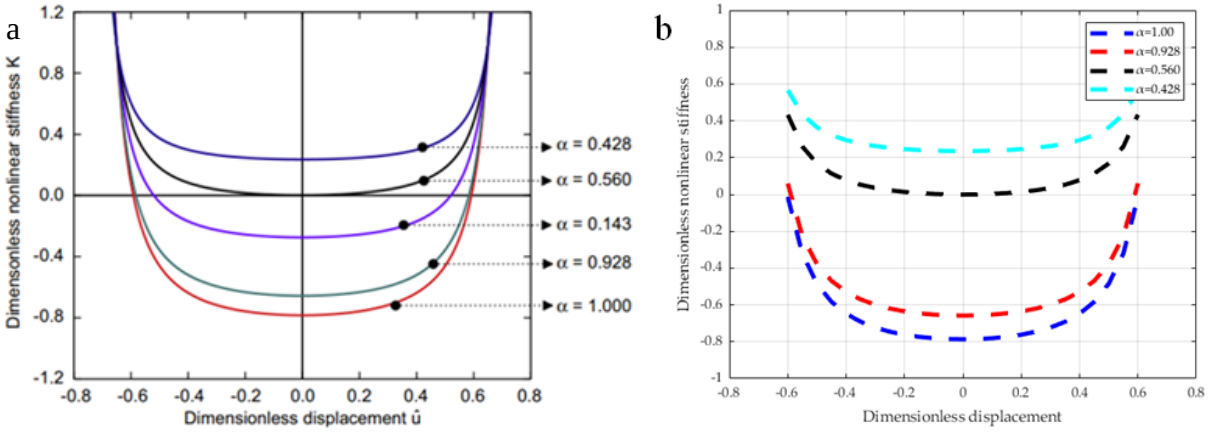

Figure 3: Validation of static characteristics for variation of α ($\gamma_1 = 0.75$, $\gamma_2 = 1.08$); a) Le and Ahn, 2013 [19], b) validation results.

As can be seen in Fig. 3, when $\gamma_1 = 0.75$ and $\gamma_2 = 1.08$, if α increases, the dimensionless nonlinear stiffness decreases and approaches zero. However, if α value is too high, the dimensionless nonlinear stiffness decreases and falls below zero.

Although various validations have been carried out in the static state, the dynamic state of the suspension also needs to be validated. For this reason, Le and Ahn's MATLAB model [19] was simulated using the Altair® Inspire program. Therefore, we validated the Altair® Inspire model using the results of Le and Ahn's MATLAB model [19] to prove its suitability. Inspire software is a very useful software for motion analysis and simulation. Thus, working problems that cannot be seen in mathematical calculations can also be observed. In the Inspire model, firstly the ground of the model was determined. This ground is a balancing factor for the suspension seat; other support elements are positioned on this ground. At the next step, the

joints on the model were defined. Inspire software can automatically detect joints in the model. The type of joints detected then whether they were active or locked were determined. Then, the process of defining the spring and damper used in the model was started. At this point, the stiffness of the horizontal and vertical springs, the springs' free length, and the damper's damping coefficient were defined. The materials of the elements used in the model were defined. Here, the material definition also gave the mass in the system. Subsequently the suspension part of the model was defined, the actuator was added to the suspension seat, which would give the vibration input. The actuator stimulates the suspension by oscillating at the desired frequency and amplitude. With the addition of the actuator, the simulation model was completed (Fig. 4).

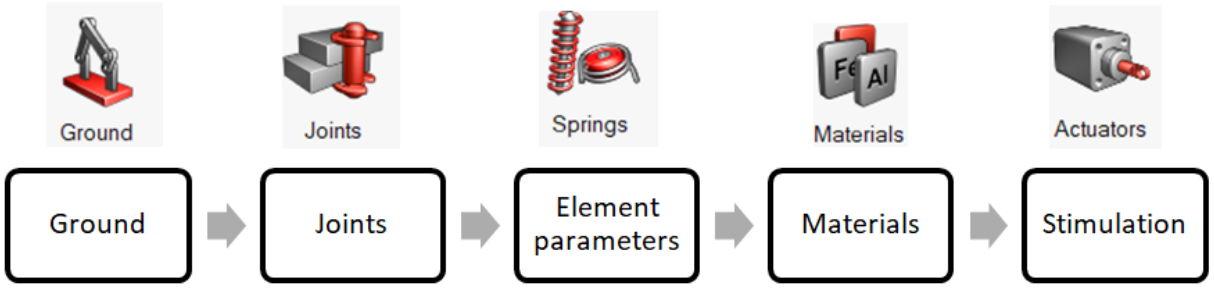

Figure 4: The Altair® Inspire model flowchart.

The system was stimulated in the 0-3 Hz frequency band for the validation study. The displacement values of the mass and the body were measured, and the transmissibility of the suspension was calculated with these values. These results composed a frequency response curve for the 0-3 Hz frequency band, which was compared with the curve in Le and Ahn's MATLAB model simulation results [19].

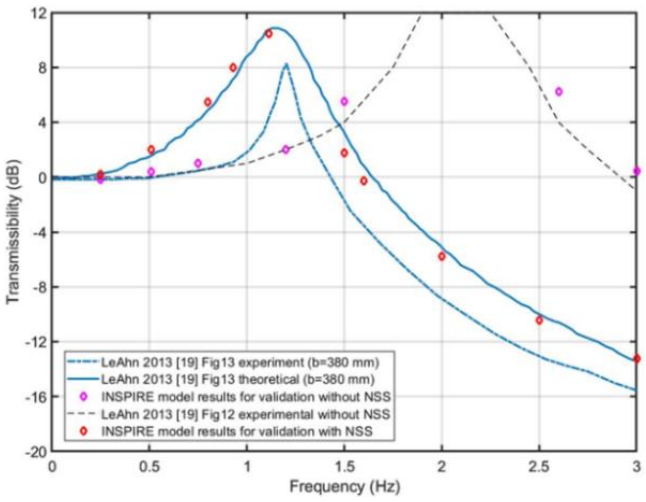

Figure 5: Comparison of the Le and Ahn study [19] and the present study.

As shown in Fig. 5, the simulation results of this study and the results of Le and Ahn's article [19] are in excellent agreement. It is almost entirely compatible with the simulation results of the relevant article. These results show that the created model works correctly. In the interviews with some companies that produce suspension seats, it was stated that the width of the seat suspension should be as small as possible; the ideal size is between 250 mm to 350 mm. For this reason, the inside width of the seat suspension was determined as 400 mm in this study. Although 400 mm is outside the specified value range, it is still an acceptable seat width. The redesigned seat suspension system model with NSS according to the size limit is presented in Fig. 6.

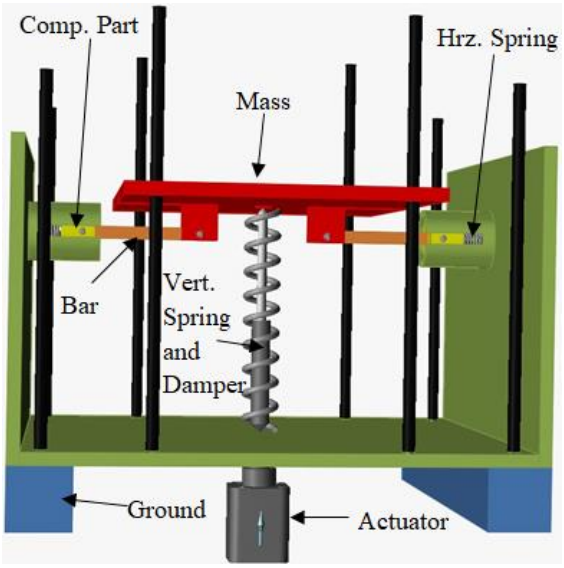

Figure 6: The Altair® Inspire model of the redesigned seat suspension system with NSS.

Parameter selection is critical for the NSS to show the expected effect. Table I shows the parameters used for the redesigned model. 75 kg dummy mass used in the study because of suspension seat manufacturers generally use this value for performance tests.

Table I: Level of parameter.

Parameter	**Values**
M	75 kg
K_v	5 N/mm
K_h	1 N/mm, 1.5 N/mm, 2 N/mm, 2.5 N/mm, 3N/mm
L_f	80 mm, 85 mm, 90 mm, 95 mm, 100 mm
B	100 mm
P	27.5 mm
	Levels
α	0.2, 0.3, 0.4, 0.5, 0.6
γ_1	1.25, 1.18, 1.11, 1.05, 1

As can be seen from Table I, the effects of changes in spring stiffness and spring preload on transmissibility (*TR*) were investigated in this study. The Taguchi method was used to understand the effect of parameter changes better. The Taguchi method is essential to reduce the number of experiments or cases [25-27]. Thus, it provides significant time and cost savings [25]. After the Taguchi process, a statistical analysis of variance (ANOVA) process was performed. After these results, the frequency response curve of the suspension seat with ideal parameter NSS and the passive suspension without NSS was compared.

3. RESULTS AND DISCUSSION

This study's Taguchi L25 series was preferred because it has 2 factors (α, γ_1) and 5 levels. Table II shows the number of cases, parameters, and *TR* results of these parameters. Absolute displacement ratios were used for transmissibility calculations. Subsequently the decibel (dB) transformation was used. Before the Taguchi analysis, the simulation results were normalized by multiplying by -1. The signal-to-noise ratio (*S*/*N*) is used in Taguchi analysis. There are three types of *S*/*N* ratio: smaller is better, larger is better, and finally nominal is best [25]. Because of the normalization process was used, larger is better was preferred.

Table II: Taguchi table and transmissibility results.

Case	α	γ_1	***TR*** (dB)	**Case**	α	γ_1	***TR*** (dB)
1	0.2	1.25	6.06	14	0.4	1.05	12.34
2	0.2	1.18	6.41	15	0.4	1.00	13.31
3	0.2	1.11	6.74	16	0.5	1.25	11.99
4	0.2	1.05	7.08	17	0.5	1.18	13.15
5	0.2	1.00	7.43	18	0.5	1.11	14.45
6	0.3	1.25	7.85	19	0.5	1.05	15.89
7	0.3	1.18	8.4	20	0.5	1.00	17.52
8	0.3	1.11	8.96	21	0.6	1.25	14.54
9	0.3	1.05	9.53	22	0.6	1.18	16.31
10	0.3	1.00	10.12	23	0.6	1.11	18.38
11	0.4	1.25	9.79	24	0.6	1.05	20.92
12	0.4	1.18	10.6	25	0.6	1.00	24.08
13	0.4	1.11	11.45				

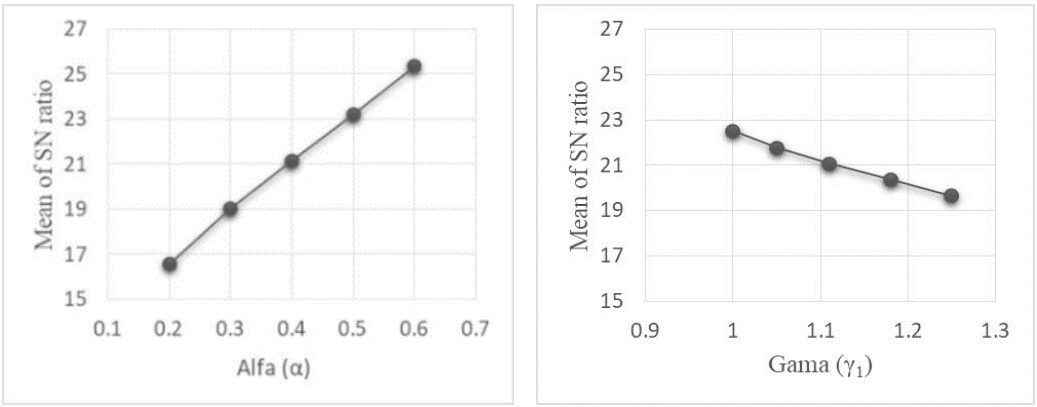

Figure 7: *S*/*N* ratio results for α and γ_1.

As shown in Fig. 7, as α increases, the *S*/*N* ratio increases. As can be seen here, the increase in the stiffness of the horizontal spring positively affects the transmissibility. Also, as γ_1 decreases, the *S*/*N* ratio increases. This means that an increase in the amount of preload on the horizontal springs decreases the transmissibility. When Table III is examined, it is seen that the α parameter is more effective than γ_1. ANOVA method was applied to the results to investigate the parameter effects in detail.

Table III : Response table for the *S*/*N* ratios for the objective.

Level	α	γ_1
1	16.56	22.5
2	19.02	21.77
3	21.16	21.06
4	23.21	20.35
5	25.37	19.64
Delta	8.81	2.86
Rank	1	2

Table IV: Analyses of variance table for means.

Source	***DF***	**Adj *SS***	**Adj *MS***	***F***	**Contribution** (%)
α	4	452.93	113.234	68.35	83.71
γ_1	4	61.60	15.401	9.30	11.39
Error	16	26.51	1.657		4.90

As can be seen in Table IV, the α is more influential parameter than γ_1. It has a very high contribution rate of 83.71 %, γ_1 contributed 11.39 %. There is an almost eight fold contribution difference between the two parameters. The error rate obtained as a result of ANOVA was 4.90 %. This result shows that the ANOVA results are pretty reliable. When all the results are examined, it is seen that the ideal parameter values are $\alpha = 0.6$, and $\gamma_1 = 1$.

In order to better understand the effect of the NSS on isolation performance of passive suspension seat, a performance comparison of a passive suspension seat without NSS and a passive suspension seat with NSS is required. For this reason, the frequency response curve for the 0-2 Hz frequency range of these two seats was examined. This frequency range was selected because of natural frequency of some human part is in this range [28]. In addition, the isolation performance of the suspension system continues to increase at each frequency after it passes the resonance frequency. For this reason, investigations in this frequency range were deemed sufficient. The frequency response curve comparison of passive suspension seat without NSS and suspension seat with NSS created with these values is shown in Fig. 8.

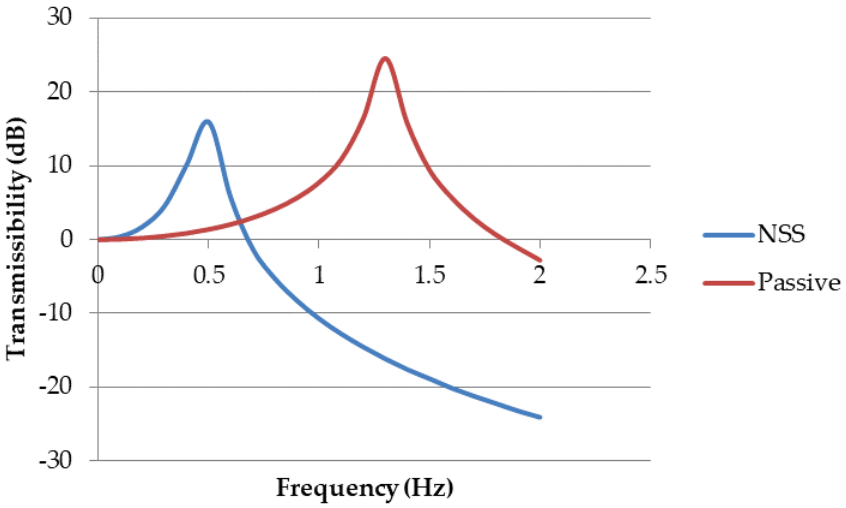

Figure 8: Transmissibility comparison of passive suspension seat without NSS vs. passive suspension seat with NSS.

When Fig. 8 is examined, it is observed that the suspension seat with NSS starts to isolate at about 0.7 Hz. On the other hand, passive suspension seat without NSS starts isolation only at about 1.9 Hz. The main reason for the natural frequency difference is the NSS. The Other parameters, stiffness of vertical spring and damping coefficient, are identical. Thus stiffness of the suspension was changed, and the starting point of isolation was taken back. There is a transmissibility difference of about nine times at 2 Hz. Between 0-0.6 Hz, the transmissibility value of passive suspension seat without NSS is lower. The reason for this is that the natural frequency of the suspension with NSS is between these values. Suspension seats are often subject to variable frequency input instead of a specific frequency input while driving. For this reason, multiple frequency inputs are essential to control the isolation performance of the seat suspension on the road. The following equation was used for the road input:

$$z_e = 8sin\big((2\pi)t\big) + 6sin\big((2\pi 1.4)t\big) + 3sin\big((2\pi 1.6)t\big) \quad \text{(mm)} \tag{10}$$

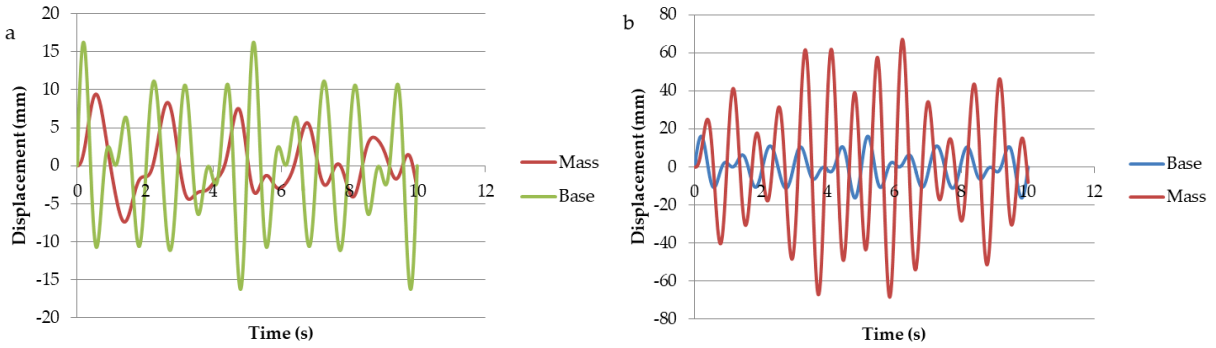

Figure 9: Response of seat suspension to road excitation; a) suspension seat with NSS, b) suspension seat without NSS.

In Fig. 9 a, the results of the suspension seat with NSS were given according to the road excitation. According to these results, suspension seat with NSS achieved good isolation all the way through. In Fig. 9 b, the results of passive suspension seat without NSS were given according to the road excitation. According to these results, passive suspension seat without NSS performed very poorly and did not provide any isolation. Last, the isolation performance of passive suspension seat with negative stiffness structure was also investigated depending on various vehicle speeds.

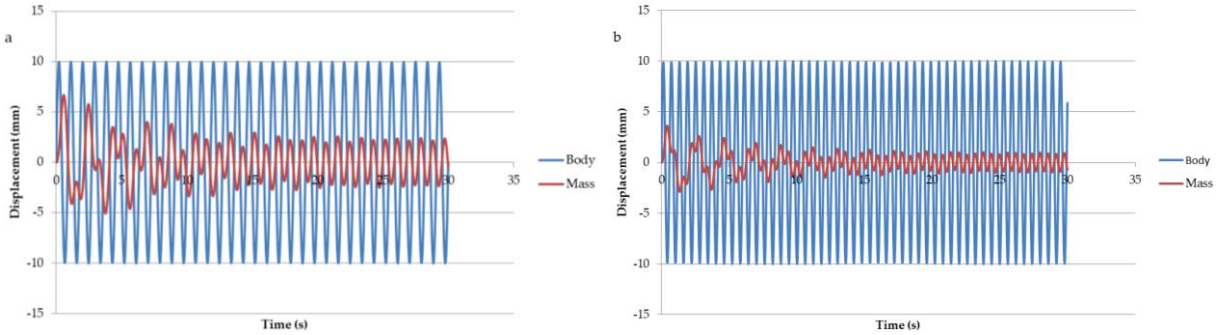

Figure 10: Isolation performance analysis; a) 40 km/h vehicle speed,10 m road period and 0.01 m road excitation amplitude, b) 60 km/h vehicle speed,10 m road period and 0.01 m road excitation amplitude.

It is clear from Fig. 10 a, b that the passive suspension seat with NSS showed a remarkable isolation performance at both speed values. In addition, it was clearly seen that the isolation performance increases as the speed increases.

4. CONCLUSIONS

In this study, the performance of an original seat suspension with NSS was considered numerically and simulated. The seat suspension model, created for the study, a significant narrowing of the width was achieved compared to the studies in the literature by moving the seat connection points. Also, the cost is low compared to active and semi-active suspension seats. Thus, this design is suitable for use on existing vehicles in view of constructive and cost. With Taguchi and ANOVA's results, it was seen that the spring stiffness ratio was more effective on transmissibility than the spring preload amount. According to ANOVA, the effect ratio of spring stiffness ratio is 83.71 %. It means that the ratio of spring stiffness is the key factor of the NSS. The study contributes to the literature by revealing this clearly. Also it was observed that the seat suspension created with the ideal negative stiffness parameters is much more effective than the passive seat suspension without NSS in term of vibration isolation. There is almost a nine times difference between isolation performance of the two suspension

types at 2 Hz frequency response. Thus, the isolation performance of suspension seat with NSS has been comparable with active and semi-active suspension seats. New suspension seat designs, which have high isolation performance, can be developed using the presented method in the study. This study will be extended via addition of different actuator types. Experimental research will be carried out to investigate the conformity of NSS to an existing driver suspension seat in future work.

ACKNOWLEDGEMENT

Mehmet Kıvanc Turan is a scholarship holder in TUBITAK 2244 – Industrial Ph.D. Fellowship Program. We would like to thank TUBITAK for their support. This study was developed within the scope of TUBITAK 118C136 and 123M189 projects.

REFERENCES

[1] Shen, Y.; Hua, J.; Fan, W.; Liu, Y.; Yang, X.; Chen, L. (2023). Optimal design and dynamic performance analysis of a fractional-order electrical network-based vehicle mechatronic ISD suspension, *Mechanical Systems and Signal Processing*, Vol. 184, Paper 109718, 13 pages, doi:10.1016/j.ymssp.2022.109718

[2] Ning, D.; Du, H.; Zhang, N.; Sun, S.; Li, W. (2020). Controllable electrically interconnected suspension system for improving vehicle vibration performance, *IEEE/ASME Transactions on Mechatronics*, Vol. 25, No. 2, 859-871, doi:10.1109/TMECH.2020.2965573

[3] Xia, X.; Ning, D.; Liu, P.; Du, H.; Zhang, N. (2023). Electrical network optimization for electrically interconnected suspension system, *Mechanical Systems and Signal Processing*, Vol. 187, Paper 109902, 18 pages, doi:10.1016/j.ymssp.2022.109902

[4] Türkkan, Y. A. (2014). *Sürüş konforu için taşıt koltuk titreşimlerinin Modellenmesi ve Analizi* (*Modelling and Analysing of Vehicle Seat Vibrations for Ride Comfort*), Master Thesis, Uludağ University, Bursa, (in Turkish)

[5] Tu, L.; Ning, D.; Sun, S.; Li, W.; Huang, H.; Dong, M.; Du, H. (2020). A novel negative stiffness magnetic spring design for vehicle seat suspension system, *Mechatronics*, Vol. 68, Paper 102370, 12 pages, doi:10.1016/j.mechatronics.2020.102370

[6] Pickard, O.; Burton, P.; Yamada, H.; Schram, B.; Canetti, E. F. D.; Orr, R. (2022). Musculoskeletal disorders associated with occupational driving: a systematic review spanning 2006-2021, *International Journal of Environmental Research and Public Health*, Vol. 19, No. 1, Paper 6837, 27 pages, doi:10.3390/ijerph19116837

[7] Kim, J. H.; Zigman, M.; Aulck, L. S.; Ibbotson, J. A.; Dennerlein, J. T.; Johnson, P. W. (2016). Whole body vibration exposures and health status among professional truck drivers: a cross-sectional analysis, *Annals of Occupational Hygiene*, Vol. 60, No. 8, 936-948, doi:10.1093/annhyg/mew040

[8] Thamsuwan, O.; Blood, R. P.; Ching, R. P.; Boyle, L.; Johnson, P. W. (2013). Whole body vibration exposures in bus drivers: a comparison between a high-floor coach and a low-floor city bus, *International Journal of Industrial Ergonomics*, Vol. 43, No. 1, 9-17, doi:10.1016/j.ergon.2012.10.003

[9] Park, M.-S.; Fukuda, T.; Kim, T.-G.; Maeda, S. (2013). Health risk evaluation of whole-body vibration by ISO 2631-5 and ISO 2631-1 for operators of agricultural tractors and recreational vehicles, *Industrial Health*, Vol. 51, No. 3, 364-370, doi:10.2486/indhealth.2012-0045

[10] Burdzik, R.; Konieczny, Ł. (2013). Research on structure, propagation and exposure to general vibration in passenger car for different damping parameters, *Journal of Vibroengineering*, Vol. 15, No. 4, 1680-1688

[11] Segla, S.; Trišović, N. (2013). Modeling and optimization of passive seat suspension, *American Journal of Mechanical Engineering*, Vol. 1, No. 7, 407-411, doi:10.12691/ajme-1-7-51

[12] Li, H.; Li, Y.; Li, J. (2020). Negative stiffness devices for vibration isolation applications: a review, *Advances in Structural Engineering*, Vol. 23, No. 8, 1739-1755, doi:10.1177/1369433219900311

[13] Zhu, S.; Tan, X.; Chen, S.; Wang, B.; Ma, L.; Wu, L. (2020). Quasi-all-directional negative stiffness metamaterials based on negative rotation stiffness elements, *Physica Status Solidi B*, Vol. 257, No. 6, Paper 1900538, 9 pages, doi:10.1002/pssb.201900538
[14] Liao, X.; Zhang, N.; Du, X.; Zhang, W. (2021). Theoretical modeling and vibration isolation performance analysis of a seat suspension system based on a negative stiffness structure, *Applied Sciences*, Vol. 11, No. 15, Paper 6928, 20 pages, doi:10.3390/app11156928
[15] Papaioannou, G.; Voutsinas, A.; Koulocheris, D.; Antoniadis, I. (2019). Dynamic performance analysis of vehicle seats with embedded negative stiffness elements, *Vehicle System Dynamics*, Vol. 58, No. 2, 307-337, doi:10.1080/00423114.2019.1617424
[16] Lee, C.-M.; Goverdovskiy, V. N.; Temnikov, A. I. (2007). Design of springs with 'negative' stiffness to improve vehicle driver vibration isolation, *Journal of Sound and Vibration*, Vol. 302, No. 4-5, 865-874, doi:10.1016/j.jsv.2006.12.024
[17] Oyelade, A. O. (2019). Vibration isolation using a bar and an Euler beam as negative stiffness for vehicle seat comfort, *Advances in Mechanical Engineering*, Vol. 11, No. 7, 10 pages, doi:10.1177/1687814019860983
[18] Le, T. D.; Ahn, K. K. (2011). A vibration isolation system in low frequency excitation region using negative stiffness structure for vehicle seat, *Journal of Sound and Vibration*, Vol. 330, No. 26, 6311-6335, doi:10.1016/j.jsv.2011.07.039
[19] Le, T. D.; Ahn, K. K. (2013). Experimental investigation of a vibration isolation system using negative stiffness structure, *International Journal of Mechanical Sciences*, Vol. 70, 99-112, doi:10.1016/j.ijmecsci.2013.02.009
[20] Le, T. D.; Ahn, K. K. (2014). Active pneumatic vibration isolation system using negative stiffness structures for a vehicle seat, *Journal of Sound and Vibration*, Vol. 333, No. 5, 1245-1268, doi:10.1016/j.jsv.2013.10.027
[21] Rahman, M.; Rahman, M. A. (2021). Application of potential energy method for driver seat suspension system using quasi-zero stiffness: a numerical and experimental study, *Jordan Journal of Mechanical and Industrial Engineering*, Vol. 15, No. 5, 431-439
[22] Ma, Z.; Zhou, R.; Yang, Q. (2022). Recent advances in quasi-zero stiffness vibration isolation systems: an overview and future possibilities, *Machines*, Vol. 10, No. 9, Paper 813, 41 pages, doi:10.3390/machines10090813
[23] Li, H.; Nguyen, V.; Xiu, Y.; Wang, C. (2023). Vibration analysis and optimization of QZSS's parameters added to the vehicle's seat suspension, *International Journal of Dynamics and Control*, Vol. 11, No. 3, 946-957, doi:10.1007/s40435-022-01067-4
[24] Zha, J.; Nguyen, V.; Ni, D.; Su, B. (2022). Optimizing the geometrical dimensions of the seat suspension equipped with a negative stiffness structure based on a genetic algorithm, *SAE International Journal of Vehicle Dynamics, Stability, and NVH*, Vol. 6, No. 2, 147-158, doi:10.4271/10-06-02-0010
[25] Turkkan, Y. A.; Aslan, M.; Tarkan, A.; Aslan, Ö.; Yuce, C.; Yavuz, N. (2023). Multi-objective optimization of fiber laser cutting of stainless-steel plates using Taguchi-based grey relational analysis, *Metals*, Vol. 13, No. 1, Paper 132, 13 pages, doi:10.3390/met13010132
[26] Visagan, A.; Ganesh, P. (2022). Parametric optimization of two point incremental forming using GRA and TOPSIS, *International Journal of Simulation Modelling*, Vol. 21, No. 4, 615-626, doi:10.2507/IJSIMM21-4-622
[27] Zseller, V.; Samu, K. (2023). Metaheuristic of arbitrary luminous intensity distribution for roadway lighting luminaires, *International Journal of Simulation Modelling*, Vol. 22, No. 3, 369-380, doi:10.2507/IJSIMM22-3-626
[28] Mandal, B. B.; Srivastava, A. K. (2006). Risk from vibration in Indian mines, *Indian Journal of Occupational & Environmental Medicine*, Vol. 10, No. 2, 53-57